Eur Biophys J (1995) 23: 399–406

European Biophysics Journal

Molecular dynamics simulations of excimer forming (+)-*anti*-BPDE-DNA adducts in aqueous solution

S. Sen[1], **A. Gräslund**[2]

[1] Department of Medical Biochemistry and Biophysics, University of Umeå, S-90187 Umeå, Sweden
[2] Department of Biophysics, Stockholm University, S-10691 Stockholm, Sweden

Received: 16 May 1994 / Accepted: 22 September 1994

Abstract. The chemical carcinogen (+)-anti BPDE preferentially binds covalently to the guanine base in the minor groove of DNA. Fluorescence spectroscopic studies have shown that the BPDE molecules bound to DNA can interact in their photo-excited state giving strong excimer fluorescence when bound to poly(dGdC) · poly(dGdC). It was suggested that the formation of such excited state complexes is most probable when the two (+)-anti-BPDE bind to guanines of adjacent base pairs on the two different strands of the DNA. In the present work a model for such an excimer forming DNA-BPDE double adduct system has been constructed and shown to be stable over a 300 ps molecular dynamics simulation in a water box. The model is a $d(CG)_3 \cdot d(CG)_3$ molecule with two BPDE molecules bound to the guanines at the 4th position on each strand, located in the minor groove and each oriented towards the 5′ end of the modified strand, respectively. The results of 300 ps MD simulation show that the two BPDE chromophores exhibited on the average a relative geometry favourable for excimer formation. The local structure at the adduct position was considerably distorted and the helix axis was bent. The modified bases were found to be paired through a stable single non-Watson Crick type of hydrogen bond.

Key words: Benzo(a)pyrene DNA adduct – Excimer – Molecular dynamics simulation

Introduction

Benzo(a)-pyrene is a well known environmental pollutant of the polyaromatic hydrocarbon group (Baum 1978; Grimmer and Pott 1983) and becomes a strong carcinogen after its metabolic activation to a highly reactive derivative benzo(a)-pyrene-7,8-dihydrodiol-9,10-epoxide (BPDE) (Dipple 1985; Thakker et al. 1985). It has been shown that the metabolic reaction can generate four different stereoisomers, (±)-syn and (±)-anti, all of which have carcinogenic activities of different degrees. In mammalian systems, the (+)-anti isomer has been identified as the most mutagenic one (Cooper et al. 1983; Jerina et al. 1991). It binds covalently to DNA. The reaction is stereo specific and the covalent binding to DNA takes place almost exclusively by a trans addition of the exocyclic amino group N2 atom of the guanine base to the C10 carbon atom of the benzylic ring of the BPDE molecule (Weinstein et al. 1978; Thakker et al. 1985).

Efforts have been made to characterize the structure of the (+)-anti-BPDE-guanine adduct in DNA by using different physico-chemical techniques (Geacintov 1988; Gräslund and Jernström 1989; Jernström and Gräslund 1994). From linear dichroism studies it has been shown that the long axis of the pyrene chromophore is oriented at an angle of less than 35° relative to the average helix axis of the DNA molecule (Geacintov et al. 1978; Undeman et al. 1983; Eriksson et al. 1988). Recently solution structures based on high resolution ^{1}H-NMR studies have been presented for (+)-anti-BPDE and the (–)-anti-BPDE bound to a DNA oligomer (Cosman et al. 1992; de Santos et al. 1992). It has been verified that in both cases the C10 atom of the BPDE molecule is bound to the guanine N2 atom situated in the minor groove. The adduct in the case of the (+)-isomer is oriented towards the 5′ end of the modified strand while, in the other case, it is oriented towards the 3′ end. In each case one face of the adduct was found to be exposed to the solvent. It was also reported that the double helical structure of the oligonucleotide was only minimally perturbed by the formation of the (+)-anti-BPDE adduct (Cosman et al. 1992). Molecular mechanical studies are in agreement with these results. For (+)-anti-BPDE it has been found that the 5′ side alignment is energetically the most favourable one and that the adduct does not cause much destabilization of the DNA structure (Rao et al. 1989; Weston et al. 1990).

Further characterization of the properties of the (+)-anti-BPDE-DNA adducts by fluorescence spectroscopy showed that strong excimer fluorescence was emit-

---

Correspondence to: A. Gräslund

ted from the bound BPDE-molecules in poly(dGdC) · poly(dGdC), while it was considerably weaker in the case of calf thymus DNA (Eriksson et al. 1988; Eriksson et al. 1990) or other synthetic polynucleotides (Eriksson et al. 1993). This observation suggested that the covalent adduct formation can occur at closely spaced guanines where the adducts can interact with each other. To probe the possible location of the excimer forming BPDE-DNA adducts, in our earlier work (Eriksson et al. 1993) we investigated different base sequences in polynucleotides, such that each sequence could give rise to a BPDE-DNA adduct pair of a particular geometry. For example, in some sequences adducts could bind to both strands, while in others they could bind only to the guanine bases on the same strand. The fluorescence spectroscopic data, supported by parallel molecular modelling and potential energy minimization calculations (in vacuum) suggested that in order to obtain a ground state geometry favouring an excimer forming BPDE-DNA adduct pair, the two (+)-anti-BPDE molecules should bind to the guanines on neighbouring base pairs in the minor groove on the different strands of the polynucleotide (Eriksson et al. 1993). It is worth mentioning here that a very similar ligand pair geometry has recently been observed in X-ray crystallographic studies of two distamycin A molecules bound in the minor groove of a DNA oligonucleotide (Chen et al. 1994).

Molecular dynamics simulation is a powerful theoretical and computational approach to the study of the structure and molecular motion of macromolecules. In our previous work we performed the potential energy minimization calculations of a double BPDE adduct in vacuum only. The pyrene chromophores of the BPDE adduct are known to be highly hydrophobic in character and their behaviour in an aqueous environment is of interest in the understanding of the geometry and effects of a double BPDE adduct on the DNA structure. In the present work we have extended our previous theoretical work (Eriksson et al. 1993) by performing an MD simulation of a model DNA-double adduct system (each adduct in its ground state) in a water box. The purpose was twofold: i) to characterize the dynamics of the double BPDE adduct and to see if the relative geometry of the adduct pair exhibits features favourable for excimer formation during dynamics in the explicit presence of water molecules and ii) to study the structural deformation of the DNA at the location of such an adduct-pair after dynamic refinement.

To our knowledge, this is the first report where the molecular dynamics of two closely bound DNA-adducts of BPDE has been addressed theoretically. Experimentally the dynamics of excimer forming BPDE adducts has previously been studied by time resolved fluorescence spectroscopy (Gräslund et al. 1992). It was found that all BPDE adducts, whether emitting fluorescence as monomers or excimers, had rapid local mobility on a subnanosecond time scale. The present simulation (300 ps) shows that the DNA-BPDE double adduct model system is a stable and well behaved chemical system on a time scale approaching the experimental one. The double helical form of the DNA remained intact over the course of the simulation but a local bending of the helix axis at the adduct-pair location was induced by the adduct pair. The two BPDE molecules resided well within the minor groove with a small portion extruded outside of the double helix. Most of the time the chromophores of the adduct pair kept closely parallel and had a significant area of overlap between them. From the comparison between MD simulations in water and in vacuum, it seems that the explicit presence of the surrounding water molecules confines the adduct pair more closely within the minor groove of the DNA and reduces their relative sliding motion.

We have also performed the MD simulations in vacuum using various starting structures differing in the relative geometry of the two adducts. The aim was to investigate to what degree the above mentioned features (parallel orientation and overlap area) are related to the input structures of the adducts.

Methods

Program and parameters

Starting structures were obtained from molecular modelling performed by the graphics package HYDRA Iris Release 1.2, Polygen Corporation England, obtained from R. Hubbard, University of York, York, UK. All potential energy minimization and molecular dynamics calculations in this study were done with the program CHARMM and the standard parameters version 19 (Brooks et al. 1983; Nilsson and Karplus 1986). The hydrogen atoms were considered explicity and the covalent bonds of the hydrogen atoms were constrained by the SHAKE (van Gunsteren and Berendsen 1977) algorithm with a tolerance of 0.0001 Å. The non-bonded interaction cutoff was set to 10 Å. A switching function was used for the non-bonded interaction terms in the range 8.0 Å to 9.0 Å so that it behaves smoothly at the cutoff point. The nonbonded pair list was updated every 10 steps. The hydrogen bond distance cutoff was set to 7.5 Å and the hydrogen bond angle cutoff was set to 100 degrees. The switching function for hydrogen bond distance was used within the range 5.5 Å to 6.5 Å. The switching function for hydrogen bond angle was used in the range 60 to 80 degrees. The hydrogen bond pair list was regenerated every 10 steps. For the dynamic simulations a time step of 1.0 fs was used. The TIP3P water model (Jorgensen 1983) was used to simulate the water molecules. For solution calculations we used a dielectric constant equal to 1.0 and included sodium counterions. In the vacuum simulation we used a distance dependent dielectric constant (Nilsson and Karplus 1986). The screening effect of the charges due to counterions was included by reducing the charges of the phosphate groups, the standard procedure for vacuum simulations.

For the (+)-anti-BPDE molecule we used the same parameters as in the previous study (Eriksson et al. 1993). We used partial atomic charges as given by Hingerty and Broyde (1985). The N2-C10 bond length was set to 1.44 Å according to Aggarwal et al. (1983), with a force constant of 350 kcal/mol $Å^{-2}$. The force constants for the dihedral and improper angles in the chromophore parts were set to a higher value of 550 kcal/mol rad^{-2} to maintain the planarity of the chromophores.

Model building

As a model of the excimer forming DNA adducts suggested by our previous work (Eriksson et al. 1993), we used a $d(CG)_3 \cdot d(CG)_3$ oligonucleotide with two (+)-anti-BPDE bound to the guanine residue at 4th position (marked by *) from the 5′ end of each strand as shown below.

5′CGCG*CG3′

3′GCG*CGC5′

To obtain a reasonable set of starting coordinates for the two excimer forming (+)-anti-BPDE adducts bound to the oligonucleotide, we used the docking facility in the graphics package HYDRA. The coordinates for the (+)-anti-BPDE molecule were taken from the crystal structure of Neidle et al. (1982). The coordinates for $d(CG)_3 \cdot d(CG)_3$ were generated as standard B-form DNA with HYDRA. Then the two (+)-anti-BPDE adduct molecules were linked to the oligonucleotide. In placing the adducts we oriented the long axis of each chromophore towards the 5′ end of its modified strand in agreement with the NMR studies on single BPDE adducts (Cosman et al. 1992). The BPDE-DNA complex was created by the patch residue technique in the CHARMM-20 (Brooks et al. 1983) package for subsequent potential energy minimization and molecular dynamics calculations.

Computational detail

Potential energy minimization protocol. To obtain an energetically suitable coordinate set for the adduct system the initial docked structure was refined according to the following protocol. First, the potential energy of the docked structure was minimized by 300 steps of the conjugate gradient minimization method in vacuum with the Powell algorithm to relax initial strains and to remove unfavourable van der Waals contacts. Ten sodium counterions were then introduced to this refined structure by placing each of them at a distance of 3.6 Å from the respective phosphorous atom on the line which starts from the phosphorous atom and bisects at the line joining the two phosphate oxygen atoms (O1 and O2) (Singh et al. 1991). To solvate the whole system it was placed in a previously equilibrated cubic water box of dimension 31.0432 Å, containing a total of 1000 TIP3P water molecules. All the water molecules with any atom closer than 2.8 Å to any atom of the DNA-adduct system were removed. Periodic boundary conditions were used by the image facility in the CHARMM program (Brooks et al. 1983). The final system consisted of a total of 2779 atoms. The resulting system was energy minimized in 500 steps of the conjugate gradient minimization method with the Powell algorithm, keeping the DNA-adduct system harmonically constrained by a force constant 20 kcal/mol $Å^{-2}$. This was done in order to allow the local adjustment of the water molecules alone to eliminate any residual geometrical strain after the removal of the overlapping water molecules (Herzyk et al. 1982; Singh et al. 1991). The potential energy of the system was then minimized further without any constraint on the solute molecule by 1000 steps for the conjugate gradient minimization method by the Powell algorithm. We did not follow any gradient criteria for these minimization processes. The final refined structure was used as the starting structure for the subsequent molecular dynamics simulations.

For energy minimization in vacuum, we minimized the potential energy of the DNA-adducts for 1000 Powell steps.

Dynamics simulation protocol. The Verlet algorithm with a 1.0 fs time step was used to calculate the classical equations of motion for the atoms during dynamics. The water box containing the DNA-double-adduct system after the energy minimization steps was first gradually heated from 98 K to 298 K during the first 1.0 ps. Every 50 fs velocities from a Gaussian distribution were given to each atom in the system. During the next 2.0 ps, equilibration was performed by assigning velocities to all atoms. The system was allowed to equilibrate further for another period of 10.0 ps without any velocity reassignment but velocity rescaling was allowed. The last two steps were subjected to a window check in the temperature range 298±5 K. The resulting system was finally allowed to follow a dynamic simulation for a further period of 287.0 ps. To keep the temperature reasonably constant, velocity rescaling was done at a frequency of 1000 steps if the average temperature was outside the range 298±5 K during this time. Over the whole period of simulation, the trajectory coordinates were saved every 200 fs for analysis. The total length of the simulation time was 300 ps including the early heating and equilibration periods and the restart facility was used as needed. The same protocol was followed for the simulation in vacuum.

Instrumentation

The graphics modelling and docking processes were performed on a Silicon Graphics Personal Iris 4D/25G workstation and the potential energy minimization and dynamics simulations were carried out on a Silicon Graphics Indigo XS24 4000 workstation. The CPU for one ps simulation in water needed about 100 min, whereas in vacuum about 9 min was needed.

Results

Energy minimization in vacuum and water

Potential energy minimization was carried out for the starting structure of a model of d(CGCG*CG) · d(CGCG*CG) with one BPDE adduct on each strand. The docking of the adducts on the DNA was done manually as described in the Methods section. The potential energy minimization calculation in aqueous solution shows that it is indeed possible to accommodate two (+)-anti BPDE adducts, bound to the nearest guanine bases on the two different strands, without breaking the double helical structure of the oligonucleotide in solution. The RMSD value between the modified energy minimized and the unmodified energy minimized d(CGCGCG) · d(CGCGCG) molecule in solution, is 1.4 Å. Figure 1 shows the energy minimized structure of the model d(CGCG*CG) · d(CGCG*CG) double adduct system in aqueous solution. A small portion of each adduct is exposed outside of the double helix. The modified base pairs appear to be quite distorted and the minor groove is widened owing to the presence of the double adducts. To estimate the width of the minor groove of the energy minimized oligonucleotide, we measured the distance between two nearest phosphorous atoms on the two strands. The distance between two such phosphorous atoms at the adducts location (e.g. GUA-5:P on one strand and CYT-11:P on the other strand) was found to be ~15.0 Å, while, in the case of an unmodified DNA molecule in solution, the distance at the same location is only ~11.3 Å.

The energy minimized structure in aqueous solution appears to be similar to the vacuum energy minimized structure. The overall RMSD value between these two structures is 0.6 Å. Two important features of the adduct pair geometry are apparent from the stereo views of the potential energy minimized structure in water – i) the planar chromophore parts of the BPDE adducts are nearly parallel to each other and ii) they have a substantial area of overlap between them. Clearly these features (in the ground state) are favourable for the excimer formation. Some parameters describing the relative geometry of the two adducts in the starting energy minimized structures in solution as well as in vacuum are given in Table 1.

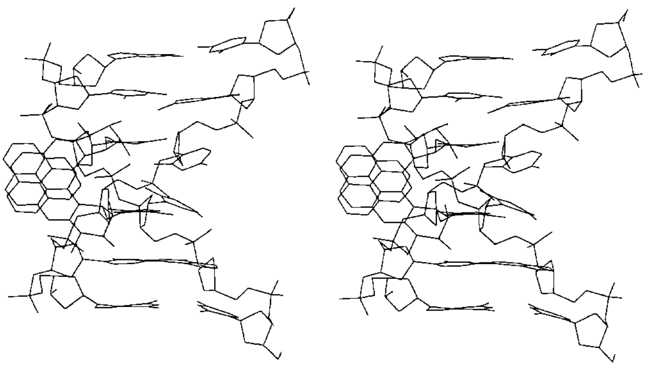

Fig. 1. Stereo view of the energy minimized structure of the model BPDE double adducts bound hexamer d(CGCG*CG) · d(CGCG*CG) in aqueous solution. The figure does not show the hydrogen atoms

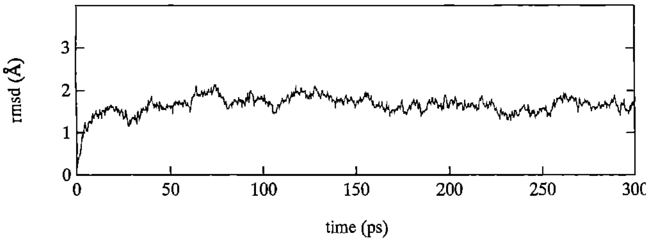

Fig. 2. The time evolution of the overall RMSD (including all atoms) of the oligomer-BPDE-adducts system

Table 1. Parameter values describing the adduct pair geometry. ρ is the projection length of the line joining the midpoints of the two chromophores on the second chromophore, θ is the angle between two vectors, each of which is normal to its respective chromophore plane and S is the average separation of the two chromophores

Structure	ρ (Å)	θ (°)	S (Å)
Energy minimized in vacuum	3.1	9.5	3.3
Energy minimized in solvent	3.2	6.0	3.1
Dynamics average structure after energy minimization	4.1	11.7	3.2

Molecular dynamics simulations in water and vacuum

We initially tried to simulate the system in the classical way i.e. without any velocity reassignment or velocity rescaling during the final part of the simulation, but subsequently found that the average temperature of the system was going down gradually during a longer simulation. Since temperature is the most important characteristic of a realistic dynamics simulation, we changed the dynamics simulation protocol and kept the temperature constant by using velocity rescaling as indicated in the methods part.

The first important result of the molecular dynamics simulation in aqueous solution is that the d(CGCG*CG) · d(CGCG*CG) double adduct system is a stable system under the dynamic conditions. The double helical structure of the oligonucleotide remained intact over the simulated time (300 ps). Bending of the helix axis at the adduct location was found to develop during the dynamics simulation, possibly to accommodate the two adducts more favourably into the minor groove.

Figure 2 shows the time evolution of the root mean square deviation (RMSD) for all atoms of the structure of the DNA-adduct pair system with respect to its starting structure at 200 fs intervals obtained from the dynamic trajectory. A rapid increase in the RMSD value in the very early part of the simulation was observed, followed by a steady value with rather small fluctuations in the case of the aqueous solution, indicating that the system has reached a steady structure.

To judge the suitability of the present model for excimer formation under dynamic conditions one should probe the relative positions of the two chromophores in their ground state. Here we have studied two quantities, i) the time evolution of the angle between the planes of the chromophores and ii) the time evolution of the area of overlap between them. The parallelism between the two chromophore planes was estimated by computing the angle (θ) between the two vectors normal to each chromophore plane in the structure (Fig. 3). Figure 4 shows the time course of the angle between the two normals on the two chromophore planes in solution (Fig. 4a) and vacuum (Fig. 4b) simulations. Most of the time the normals make an angle

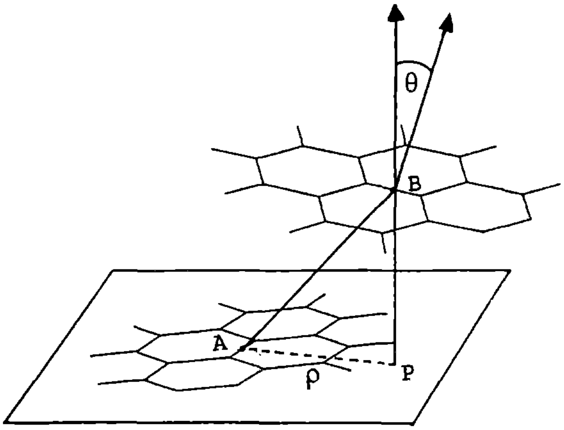

Fig. 3. Schematic description of the geometric quantities (θ) and (ρ). (θ) represents the angle between the vectors normal to each BPDE chromophore plane and (ρ) represents the projection length (AP) of the line (AB) joining the two midpoints (A and B) of the two chromophores on the second chromophore plane

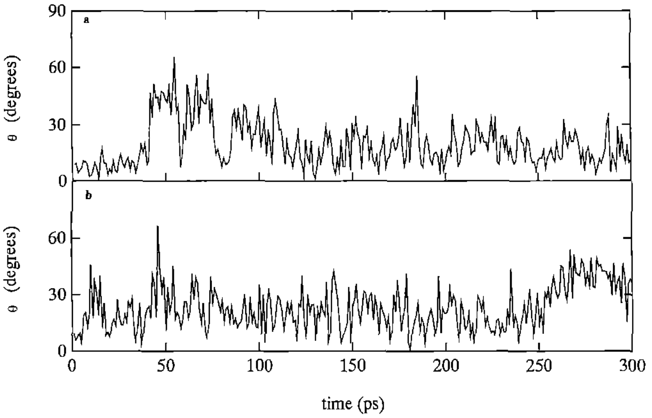

Fig. 4. **a** The time evolution of the angle (θ) between the two vectors normal to the two BPDE chromophore planes, during MD simulation in aqueous solution. **b** The same in vacuum simulation

less than 30° with an average of 20°. To estimate a parameter describing the area of overlap we have calculated the length (ρ) of the projection of the line joining the mid points of the two chromophores on the second chromophore (Fig. 3). Figure 5 demonstrates the time evolution of this quantity in solution (Fig. 5a) and vacuum (Fig. 5b) simulations. As the longest distance between two atoms in the chromophore part of the BPDE molecule is about 6.8 Å, one can expect some area of overlap if the projection length (ρ) is less than this distance. It is clear from Fig. 5 that most of the time during the solution simulation, the two chromophores move relative to each other keeping the projection length (ρ) within the range 3–5 Å (<6.8 Å), indicating a fair degree of area of overlap. The time evolution of (θ) and (ρ) over the simulated time indicate that the two BPDE adducts are fairly mobile. Their relative movement includes sliding as well as tilting limited mainly in the ranges 0°–30° for (θ) and 3–5 Å for (ρ). Both adducts were always found to be mainly within the minor groove with only a portion protruding outside it. Comparing the sliding movements of the two adducts from Fig. 5 it seems that the explicit presence of water molecules in the solution simulation reduced the sliding of the adducts relative to that in vacuum.

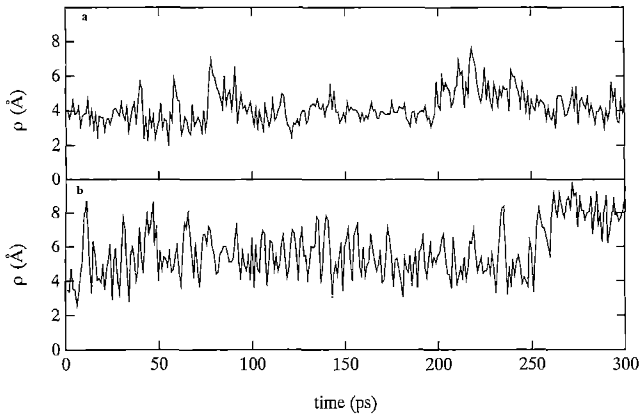

Fig. 5. **a** The time evolution of the projection length (ρ) of the line joining the midpoints of the two BPDE chromophores, on one of the chromophores, during MD simulation in aqueous solution. **b** The same in vacuum simulation

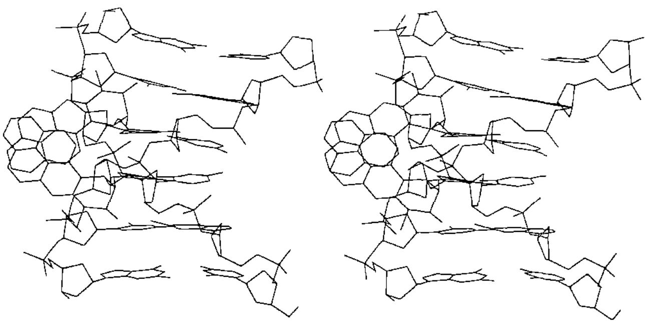

Fig. 6. Stereo view of the energy minimized dynamic average structure of the system over the last 150 ps MD simulation in aqueous solution

To estimate the average structural features, the average structure of the model over the last 150 ps of the solution simulation trajectory was calculated using CHARMM and the structure was energy minimized over 500 steps of Powell algorithm (Fig. 6). The parameter values (ρ and θ) describing the relative geometry of the two adducts in this average structure are given in Table 1. Clearly the average structure has all the structural features favourable for excimer formation. We also estimated the average separation between the two planar chromophores in the average structure simply by calculating the normal distance of each atom on one chromophore plane from the plane of the other chromophore and then taking the average. The average separation was found to be 3.2 Å. The chromophore plane separation in the case of free BPDE excimers has been found to be about 3.4 Å (Prout and Wright 1968; Birks 1980).

The base pairing at the adduct-pair location in this average structure was found to be considerably distorted. The presence of the double adduct apparently made these complementary bases incapable of forming the usual Watson-Crick (W-C) base pairs. Instead, they were found to be capable of making one different hydrogen bond. The CYT-9:O2 is hydrogen bonded with GUA-4:HN1 (bond length 2.6 Å and bond angle 166.2°). Similar H-bonding occurs between CYT 3 and GUA 10 (bond length 2.7 Å and bond angle 161.9°). It should be noted that the GUA:HN1-CYT:02 H-bond is not of the usual W-C type, where GUA:HN1 is H-bonded with CYT:N3. Similar H-bonds were found also for the other BPDE adduct. We studied the time evolution of the distance (Fig. 7a) and the angle (Fig. 7b) between the acceptor and donor of the H-bond between CYT-9:O2 and GUA-4:HN1. The results show that the bond length of the single hydrogen bond in the distorted base pairs fluctuates within the range 2.4 Å – 3.1 Å with an average 2.70 Å and keeps a close linearity with the angle fluctuating within the range 140° – 180° with an average 160.0°. These results indicate that although this is not a normal Watson-Crick type hydrogen bonding, it is still a relatively strong and stable bond which was maintained throughout the dynamics simulation. The distortion of base pairs was found to be localized mainly to the BPDE-adduct modified base pairs. The other base pairs were found to maintain the usual Watson-Crick base pairing. Figure 8 shows snap shots of the oligonucleotide-double adduct system from the molecular dynamics trajectory in the solvent simulation, at 100 ps, 200 ps and 300 ps.

Finally we studied the behaviour during vacuum MD simulations of the DNA-adducts with different starting geometries, although with the general orientation towards the 5′ end of each modified strand. These starting geometries were characterized by the (θ) and (ρ) values of the adducts pair in each structure. The (θ) and (ρ) values in the initial and final average structures (over the last 50 ps of the 100 ps MD simulation) in each case are summarized in Table 2 (structures 1–12). Clearly most of these structures show average features favourable for excimer formation. There is no obvious correlation between input and average dynamic structure. It should be pointed out that the narrow width of the minor groove and the covalent bonding of each adduct to the respective guanine base restricted the possible choices of relative geometry between the adducts. Efforts to prepare a starting adduct pair geometry with a wide angle between the adducts resulted in bad van der Waal contacts with the DNA backbone atoms and as a result the energy minimization and MD calculations were not possible. Structures 13–14 in Table 2 were constructed with each adduct oriented towards the 3′ end of the respective strand. These structures keep the general orientation during the simulation, but show higher energy that structures 1–12.

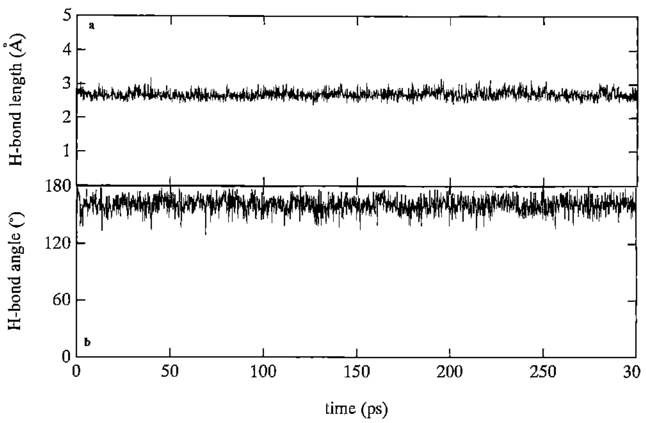

Fig. 7. a The time evolution of the H-bond length GUA:N1 (-H1)–CYT:O2 for one of the adduct modified base pairs. **b** The time evolution of the H-bond angle GUA:N1(-H1)–CYT:O2 for one of the adduct modified base pairs

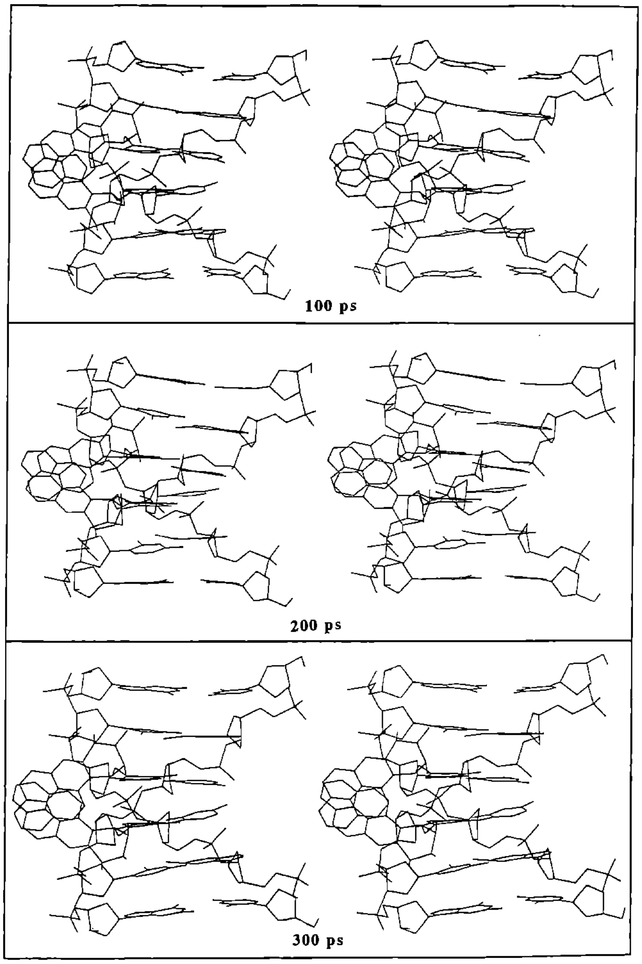

Fig. 8. Snap shots at 100ps, 200ps and 300ps from the dynamics trajectory of the MD simulation in a water box

Discussion

We have performed potential energy minimization and molecular dynamics simulations on a DNA-BPDE adduct model with two adducts on consecutive base pairs on opposite strands, in water and in vacuum. The model should be relevant to BPDE adduct pairs in consecutive GC base pairs which are manifested through excimer fluorescence in the excited state. It is well known that the present methods of potential energy minimization usually lead to the

Table 2. Parameter values describing the starting and the average adduct pair geometries in vacuum MD simulations using different starting structures. θ_i and θ_a are the values of the angle between the two pyrene planes in the initial geometry (i) and the geometry of the dynamics average (a). ρ_i and ρ_a are the respective values for the projection length

Model	θ_i (°)	θ_a (°)	ρ_i (Å)	ρ_a (Å)	E_i kcal/mol	E_a kcal/mol
1	19.9	8.8	3.3	3.2	–237.7	–323.9
2	25.7	14.1	4.0	4.4	–238.6	–345.1
3	13.8	20.4	5.9	4.6	–231.8	–270.6
4	17.3	26.5	8.7	5.4	–228.6	–329.3
5	37.0	11.9	7.3	3.7	–240.7	–316.5
6	3.9	28.0	5.4	9.4	–250.9	–329.5
7	11.8	21.8	5.5	4.6	–237.6	–323.3
8	15.7	18.7	7.7	6.2	–247.2	–340.9
9	26.7	32.7	6.1	8.5	–234.3	–328.1
10	17.8	23.8	2.6	5.1	–238.0	–284.6
11	20.8	25.5	5.0	5.5	–238.4	–313.2
12	27.7	31.9	7.0	6.0	–238.1	–316.6
13	43.0	55.8	14.8	14.5	–178.2	–204.5
14	39.1	58.2	14.6	14.9	–198.3	–233.4

nearest local minimum. Therefore we did not follow any rigid RMS energy gradient criteria for energy minimization. The purpose was to obtain an energetically favourable initial structure of the DNA-BPDE double adducts model system for the subsequent MD calculations.

For the formation of an excimer in a covalently restrained system, a substantial area of overlap and a close parallel positioning of the interacting chromophores already in the ground state are favourable because such an excited state complex is formed by a charge transfer reaction through the overlapping π-electronic clouds of the two chromophores (Turro 1978). The potential energy minimized structure in water shows that in our model system, even in the ground state, the two adduct chromophores have a considerable amount of area overlap and rather parallel orientation favourable for excimer formation (Fig. 1). Moreover, during the dynamics over the simulated time, the system was found to be stable (Fig. 2). The two chromophores exhibited some tilting movement (Fig. 4) and also a sliding motion relative to each other (Fig. 5). These relative motions were found to be limited within a reasonable range, allowing the chromophore pairs to maintain the two features favourable for excimer formation. Moreover, in this model the average separation between the chromophore planes of the adducts are consistent with the separation value relevant for the case of freely diffusing pyrene molecules exhibiting excimer fluorescence.

The double BPDE adduct seems to affect the geometry of the associated base pairs more than has been found for a single BPDE adduct. In a single adduct case the modified base pair was found to remain essentially intact in the solution structure determined by NMR (Cosman et al. 1992) in agreement with calculations (Singh et al. 1991). Here, for the double adducts, we find that the modified base pairs are highly distorted. Each of the modified base pairs is paired by one unusual but rather stable H-bond between GUA:NH1 and CYT:O2 (Fig. 7). A bending of the helix axis at the location of the adducts was developed, possibly to accommodate the double adducts.

We have also studied the vacuum dynamics of several starting structures with different relative geometries of the two adducts. The results show that the energy minimized dynamics average structure was independent on the starting parameters in a reasonably wide range.

Excimer fluorescence in BPDE-modified DNA may be considered as a probe for adduct formation in two neighbouring base pairs. Experimental evidence for DNA structure deformation upon BPDE-adduct formation has demonstrated a decrease in persistence length (Eriksson et al. 1988), DNA bending (Mao et al. 1993), and local widening of the minor groove (Singh et al. 1991; Cosman et al. 1992). All these results are presumably associated with single adducts. The results presented here show that a double adduct is expected to cause more pronounced local deformations of the DNA. The apparent loss of two H-bonds in the modified GC base pair should result in a significantly destabilized helix (with disturbed base stacking properties). At the present time, it is not known whether a double BPDE adduct is associated with any particular biological effect of BPDE. However, the present results show that in sequences allowing this type of modification, the structural deformation of the DNA should be different from sites with a mono adduct of BPDE. This is one of the possible sources of heterogeneity in DNA structure deformation, that may be at least partially responsible for the subtle base sequence dependent patterns of BPDE induced mutations in mammalian cells (Carothers and Grunberger 1990; Jernström and Gräslund 1993).

Conclusions

The present study has demonstrated the feasibility of the system d(CGCG*CG) · d(CGCG*CG) as a model of an excimer forming DNA-BPDE double adduct geometry. The molecular dynamics simulation in water over a total of 300 ps shows that the proposed structure was stable over the simulated time and exhibited relative geometry favourable for excimer formation.

It is possible to accommodate two (+)-anti-BPDE adducts bound to the nearest guanine bases on the two different strands within a widened minor groove of the polynucleotide. The energy minimized average dynamic structure shows that the base pairs involving the adducts are considerably distorted, and are paired through a single non-Watson-Crick type hydrogen bond formed between the N1 of the modified GUA and O2 of the complementary CYT base in each adduct.

Acknowledgements. We are grateful to Dr. L. Nilsson of the Karolinska Institute for useful suggestions regarding MD calculations. We are also grateful to J. Zdunek for generous help and also for providing us with his graphics packages GIPSY for preparing the diagrams. This work was financially supported by the Natural Sciences Computational Fund, University of Umeå, the Swedish Work Environmental Fund, The Swedish Natural Science Research Council and Magn. Bergwall's Foundation.

References

Aggarwal AK, Islam SA, Neidle S (1983) Computer modelling studies of the covalent interactions between DNA and the enantiomers of anti-7,8-diol, 9,10-epoxy-benzo(a)pyrene. J Biomol Struct Dynam 1:873–881

Baum EJ (1978) Occurrence and surveillance of polycyclic aromatic hydrocarbons. In: Polycyclic Aromatic Hydrocarbons and Cancer. Vol 1, Gelboin HV, Ts'o POP (eds) Academic Press, New York, pp 45–62

Birks JB (1980) Photophysics of Aromatic Molecules Wiley, New York

Brooks R, Bruccoleri RE, Olafson BD, States DJ, Swaminathan S, Karplus M (1983) A program for macromolecular energy, minimization and dynamics calculations. J Comput Chem 4:187–217

Carothers AM, Grunberger D (1990) DNA base changes in benzo(a) pyrene diol epoxide induced dihydrofolate reductase mutants of Chinese hamster ovary cells. Carcinogenesis 11:189–192

Chen X, Ramakrishnan B, Rao ST, Sundaralingam M (1994) Binding of two distamycin A molecules in the minor groove of an alternating B-DNA duplex. Struct Biol 1:169–175

Cooper CS, Grover PL, Sims P (1983) The metabolism and activation of benzo(a) pyrene. In: Bridges JW, Chasseaud LF (eds) Prog Drug Metab 7:295–396

Cosman M, de los Santos C, Fiala R, Hingerty BE, Singh SB, Ibanez V, Margulis LA, Live D, Geacintov NE, Broyde S, Patel DJ (1992) Solution conformation of the major adduct between the carcinogen (+)-anti-benzo(a) pyrene diol epoxide and DNA. Proc Natl Acad Sci, USA 89:1914–1918

de los Santos C, Cosman M, Hingerty BE, Ibanez V, Margulis LA, Geacintov NE, Broyde S, Patel DJ (1992) Influence of benzo(a)pyrene diol epoxide chirality on solution conformations of DNA covalent adducts: the (–)-trans-anti-(BP)G.C adduct structure and comparison with the (+)-trans-anti-(BP)G.C enantiomer. Biochemistry 31:5245–5252

Dipple A (1985) Polycyclic aromatic hydrocarbon carcinogenesis. An introduction. In: Polycyclic Hydrocarbons and Carcinogenesis: Harvey RG (ed) ACS Symposium series 238; American Chemical Society: Washington DC, pp 1–17

Eriksson M, Norden B, Jernström B, Gräslund A (1988) Binding geometries of benzo(a)pyrene-diol epoxide isomers covalently bound to DNA. Orientational distribution. Biochemistry 27: 1213–1221

Eriksson M, Norden B, Jernström B, Gräslund A, Lycksell P-O (1988) Observation of excimer formation in the covalent adducts of 9,10-epoxy-7,8,9,10-tetrahydrobenzo(a)pyrene-7,8-diol with poly(dG-dC). J Chem Soc Chem Commun 1988:211–212

Eriksson M, Eriksson S, Jernström B, Norden B, Gräslund A (1990) Excimer fluorescence of (+)-anti-benzo(a) pyrene diol epoxide covalently bound to poly (dG-dC): Structural Implications. Biopolymers 29:1249–1258

Eriksson M, Kim SK, Sen S, Gräslund A, Jernström B, Norden B (1993) Location of excimer-forming adducts of (+)-anti-benzo(a) pyrene diol epoxide in DNA. J Am Chem Soc 115:1639–1644

Geacintov NE (1988) Mechanisms of reaction of polycyclic aromatic epoxide derivatives with nucleic acids. In: Polycyclic Aromatic Hydrocarbon Carcinogenesis: Structure-Activity Relationships vol. 2, Yang SK, Silverman BD (eds) CRC: Boca Raton, FL, pp 181–206

Geacintov NE, Gagliano AG, Ivanovic V, Weinstein IB (1978) Electric linear dichroism study on the orientation of benzo(a) pyrene-7,8-dihydrodiol 9,10-epoxide covalent adduct to DNA. Biochemistry 17:5256–5262

Gräslund A, Jernström B (1989) DNA-carcinogen interaction: covalent DNA-adducts of benz(a) pyrene 7,8-dihydrodiol 9,10-epoxides studied by biochemical and biophysical techniques. Q Rev Biophys 22:1–37

Gräslund A, Kim SK, Eriksson S, Norden B, Jernström B (1992) Dynamics of benzo(a)pyrene diol epoxide adducts in poly(dG-dC) · (dG-dC) studied by synchrotron excited fluorescence polarization anisotropy decay. Biophys Chem 44:21–28

Grimmer G, Pott F (1983) In: Environmental Carcinogens: Polycyclic Aromatic Hydrocarbons, Grimmer G (Ed) CRC Press, Boca Raton, FL, p 61

Herzyk P, Neidle S, Goodfellow JM (1992) Conformations and dynamics of drug-DNA interactions. J Biomol Struct Dynam 10: 97–139

Hingerty BE, Broyde S (1985) Carcinogen – base stacking and base – base stacking in dCpdG modified by (+) and (–) anti-BPDE. Biopolymers 24:2279–2299

Jerina DM, Chadha A, Cheh A, Schurdak ME, Wood AW, Sayer JM (1991) In: Biological Reactive Intermediates. Witmer CM, Snyder R, Jollow DJ, Kalf GS, Kocsis JJ, Sipes IG (eds) Plenum Press, New York, p 533

Jernström B, Gräslund A (1994) Covalent binding of benzo(a) pyrene 7,8-dihydrodiol 9,10-epoxides to DNA: molecular structures, induced mutations and biological consequences. Biophys Chem 49:185–199

Jorgensen WL, Chandrasekhar J, Madura JD, Impey RW, Klein ML (1983) Comparison of simple potential functions for simulating liquid water. J Chem Phys 79:926–935

Mao B, Li B, Li D, Geacintov NE (1993) Characteristics of stereospecific N^2-dG-BPDE-oligonucleotide adducts: flexible hinge joints and differences in exonuclease digestion efficiencies. J Biomol Struct Dynam 10:a123

Neidle S, Subbiah A, Kuroda R, Cooper CS (1982) Molecular structure of (±)-7,8,9,10 tetrahydroxy-7,8,9,10-tetrahydrobenzo(a) pyrene determined by X-ray crystallography. Cancer Res 42: 3766–3768

Nilsson L, Karplus M (1986) Energy functions for energy minimization and dynamics of nucleic acids. J Comput Chem 7:591–616

Prout VCK, Wright JD (1968) Betrachtungen zu den Kristallstrukturen von Electronen-donor-acceptor-komplexen. Angew Chem 80:688–697

Rao SN, Lybrand T, Michau D, Jerina DM, Kollman PA (1989) Molecular mechanics simulations on covalent complexes between polycyclic carcinogens and B-DNA. Carcinogenesis 10:27–38

Singh SB, Hingerty BE, Singh UC, Greenberg JP, Geacintov NE, Broyde S (1991) Structures of the (+)- and (–)-trans- 7, 8-dihydroxy -anti-9,10-epoxy-7,8,9,10-hydrobenzo(a) pyrene adducts to guanine-N^2 in a duplex dodecamer. Cancer Res 51:3482–3492

Thakker DR, Yagi H, Levin W, Wood AW, Conney AH, Jerina DM (1985) Polycyclic aromatic hydrocarbons: metabolic activation to ultimate carcinogens. In: Bioactivation of Foreign Compounds. Anders MW (ed) Academic Press, New York, pp 177–242

Turro NJ (1978) Modern Molecular Photochemistry. The Benjamin Cumming's, Menlo Park, pp 135–146

Undeman O, Lycksell PO, Gräslund A, Astlind T, Ehrenberg A, Jernström B, Tjerneld F, Norden B (1983) Covalent complexes of DNA and two stereoisomers of benzo(a) pyrene-7,8-diyhydrodiol-9,10-epoxide studied by fluorescence and linear dichroism. Cancer Res 43:1851–1860

van Gunsteren WF, Berendsen HJC (1977) Algorithms for macromolecular dynamics and constraint dynamics. Mol Phys 34: 1311–1327

Weinstein IB, Jeffrey AM, Leffler S, Pulkrabek P, Yamasaki H, Grunberger D (1978) Interactions between polycylic hydrocarbons and cellular macromolecules. In: Polycyclic Hydrocarbons and Cancer, vol 2. Gelboin HV, Ts'o POP (eds) Academic Press, New York, pp 3–36

Weston A, Newman MJ, Mann DL, Brooks BR (1990) Molecular mechanisms and antibody binding in the structural analysis of polycyclic aromatic hydrocarbon-diol-epoxide-DNA adducts. Carcinogenesis 11:859–864